Controlling dissipative and Hamiltonian chaos by a constant periodic pulse method

Haibo Xu,[1,2,*] Guangrui Wang,[2] and Shigang Chen[2]
[1]*Graduate School, China Academy of Engineering Physics, P.O. Box 2101, Beijing 100088, People's Republic of China*
[2]*Center for Nonlinear Studies, Institute of Applied Physics and Computational Mathematics, P.O. Box 8009-28, Beijing 100088, People's Republic of China*

(Received 17 July 2000; revised manuscript received 1 March 2001; published 12 June 2001)

A constant periodic pulse method is proposed to control dissipative and Hamiltonian chaos. Using the convergence of the chaotic orbit in finite time, the stable segment of the chaotic orbit that satisfies the desired dynamical features can be made to form a closed orbit by the action of a proper perturbation on the system variables. A way to determine the intensity of the perturbation and the corresponding fixed points is presented. The method is robust against the presence of external noise.

DOI: 10.1103/PhysRevE.64.016201 PACS number(s): 05.45.−a

I. INTRODUCTION

A wide variety of methods have been proposed for controlling chaos in nonlinear dynamical systems since Ott, Grebogi, and Yorke (OGY) proposed to apply a small perturbation to stabilize an unstable periodic orbit [1]. However, much of the work in the literature so far has concentrated on dissipative systems [2–4], where the periodic pulse method, in which proportional pulses act on the system variables, is one method used [5,6]. For conservative systems, there are only a few methods [7–9]. This might be because there are no chaotic attractors. Therefore, the initial condition acts as a special controlling parameter in describing the chaotic behavior. In this paper, we propose a constant periodic pulse method in which the periodic pulse is independent of the system variables. The method is suitable for both dissipative and conservative systems. The procedure is as follows. First, we calculate the finite time Lyapunov exponents [10] (also called the local Lyapunov exponents) for initial points distributed uniformly in the phase space, and obtain the finite time convergence zones in different time lengths. Then we select the stable segment that satisfies the desired dynamical features, and determine the intensity and interval of the perturbation. When the system approaches the end point of the desired orbit, we act the perturbation on the system variables to make the system return to the neighborhood of the initial point. By successive action of the constant periodic perturbation, the stable segment of the chaotic orbit can be made to form a closed periodic orbit. This method can stabilize nonlinear dynamical systems into any desired periodic orbit and does not require any previous knowledge of the system. We have studied the use of the constant periodic pulse method in one-dimensional dissipative systems [11]. Here, we illustrate the method with the Hénon and standard maps and the Hénon-Heiles model, representing discrete dissipative, discrete, and continuous conservative systems, respectively. We also discuss the effect of Gaussian white noise and find that our method is robust against the presence of external noise.

The outline of the rest of the paper is as follows. In Sec. II we present the constant periodic pulse method. Numerical results for the Hénon map, the standard map, and the Hénon-Heiles model are presented in Sec. III. In Sec. IV we briefly study the effect of external noise. Finally, the main results of this paper are discussed and summarized in Sec. V.

II. THE CONSTANT PERIODIC PULSE METHOD

We consider the discrete time dynamical system

$$\mathbf{x}_{n+1}=\mathbf{F}(\mathbf{x}_n), \tag{1}$$

where $\mathbf{x}\in\mathbb{R}^N$ and $\mathbf{F}$ is a sufficiently smooth function of $\mathbf{x}$.

There is a close relationship between the controllability and predictability in finite time for a dynamical system. The latter depends not only on the precision of measurement, but also on the stability of the system. For a chaotic orbit, there may be large changes in local stability, which can be expressed by local Lyapunov exponents.

We iterate $\mathbf{x}_s$ T times to get

$$\mathbf{x}_{s+T}=\mathbf{F}^{(T)}(\mathbf{x}_s). \tag{2}$$

The convergence after T iterations from the neighborhood of point $\mathbf{x}_s$ can be described by the Jacobian matrix of Eq. (2),

$$D\mathbf{F}^{(T)}(\mathbf{x}_s)=\frac{\partial\mathbf{F}(\mathbf{x}_{s+T-1})}{\partial\mathbf{x}_{s+T-1}}\frac{\partial\mathbf{F}(\mathbf{x}_{s+T-2})}{\partial\mathbf{x}_{s+T-2}}\cdots\frac{\partial\mathbf{F}(\mathbf{x}_s)}{\partial\mathbf{x}_s}. \tag{3}$$

This is an $N\times N$ matrix. If the map or dynamical equation describing the system is not known, the matrix may be determined by local linear fitting at point $\mathbf{x}_s$. We can define the finite time Lyapunov exponents $\Lambda_i(\mathbf{x}_s,T)$ of T iterations from $\mathbf{x}_s$ for the map (1) as

$$\Lambda_i(\mathbf{x}_s,T)=\frac{1}{T}\ln|\lambda_i(\mathbf{x}_s,T)| \quad (i=1,2,\ldots,N). \tag{4}$$

Here $\lambda_i(\mathbf{x}_s,T)$ are the eigenvalues of the Jacobian matrix (3). For conservative systems, the Jacobian matrix often exhibits complex-conjugate eigenvalues at one or more of the orbit points. In this case, $|\lambda_i(\mathbf{x}_s,T)|$ are always equal to 1. $\Lambda_i(\mathbf{x}_s,T)$ reflect the stability of the segment of the chaotic orbit after T iterations in the neighborhood of point $\mathbf{x}_s$. If T is very large, the largest finite time Lyapunov exponent

*Email address: haiboxu65@hotmail.com

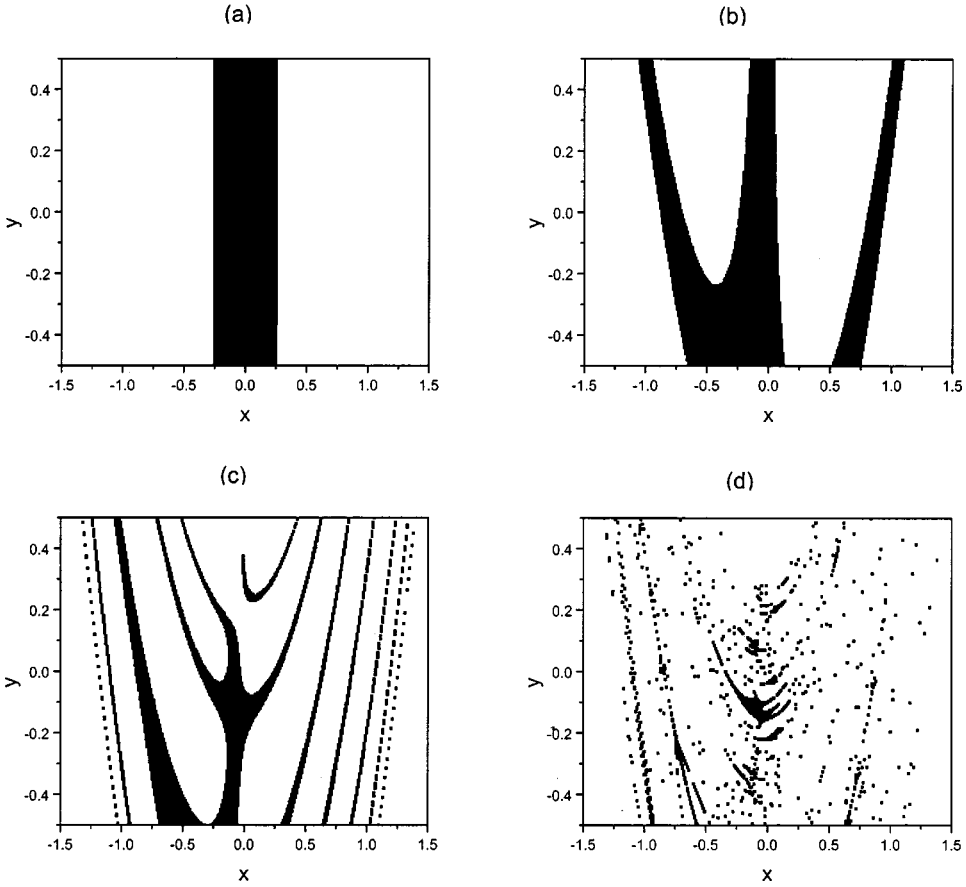

FIG. 1. The finite time convergence zones of different iterations for the Hénon map. (a) 1; (b) 2; (c) 4; (d) 10.

$\Lambda_{\max}(\mathbf{x}_s,T)$ plays a dominant role. $\Lambda_i(\mathbf{x}_s,T)$ approaches the limiting value in the form of T^{-p} as $T\to\infty$ (p is a constant for a given system) [12]. The usual Lyapunov exponents are $\Lambda_i=\lim_{T\to\infty}\Lambda_i(\mathbf{x}_s,T)$, which are independent of the initial conditions. The orbit is stable if

$$\Lambda_i(\mathbf{x}_s,T)\leqslant 0 \quad (i=1,2,\ldots,N). \tag{5}$$

In controlling chaos, we are interested in the set of all initial points $\mathbf{x}_s$ that satisfy $\Lambda_i(\mathbf{x}_s,T)\leqslant 0$. Generally, the set of $\mathbf{x}_s$ forms a many-part region in phase space which have nonzero measurement and do not link to each other. This region is called the finite time convergence zone. We examine the orbits starting from different initial points in the region, and select a stable segment of the chaotic orbit containing $T+1$ points $\mathbf{x}_s,\mathbf{x}_{s+1},\ldots,\mathbf{x}_{s+T}$ where the first T points satisfy the desired dynamical behavior. Since $\mathbf{x}_s\neq\mathbf{x}_{s+T}$, this orbit is not a periodic orbit. Our intention is to make a stable segment of the orbit that satisfies the desired dynamical features form a closed orbit by the action of a proper perturbation on the system variables without affecting its convergence. Thus, when the system falls in the neighborhood of $\mathbf{x}_{s+T}$, we let a constant perturbation determined by

$$\mathbf{p}_0=\mathbf{x}_s-\mathbf{x}_{s+T} \tag{6}$$

act on the system variables. Let the T iterations of the map starting from $\mathbf{x}_s$ return back to $\mathbf{x}_s$:

$$\mathbf{x}^*_{s+T}=\mathbf{F}^{(T)}(\mathbf{x}_s)+\mathbf{p}_0=\mathbf{x}_{s+T}+\mathbf{p}_0=\mathbf{x}_s. \tag{7}$$

Repeating the above process by successive periodic pulses on the system variables, the map (1) is replaced by

$$\mathbf{x}_{n+1}=\mathbf{F}(\mathbf{x}_n)+\mathbf{p}_{0_n}=\mathbf{F}(\mathbf{x}_n)+p_0\sum_{m=m_0}^{\infty}\delta(n-mT), \tag{8}$$

TABLE I. The initial points, end point, and intensities of periodic pulses for four different orbits of the Hénon map

T	x_s	y_s	x_{s+T}	y_{s+T}	p_{0_x}	p_{0_y}	p_x	p_y
1	0.150	0.205	1.173 50	0.045 00	1.023 50	0.160 00	−1.003	0.130
2	−0.960	0.360	0.705 19	0.020 93	−1.665 19	0.339 07	−1.635	0.315
4	−0.055	−0.125	−1.220 39	0.375 81	1.165 39	−0.500 81	1.145	−0.475
10	−0.092	−0.105	−1.061 48	0.366 95	0.969 48	−0.471 95	0.950	−0.460

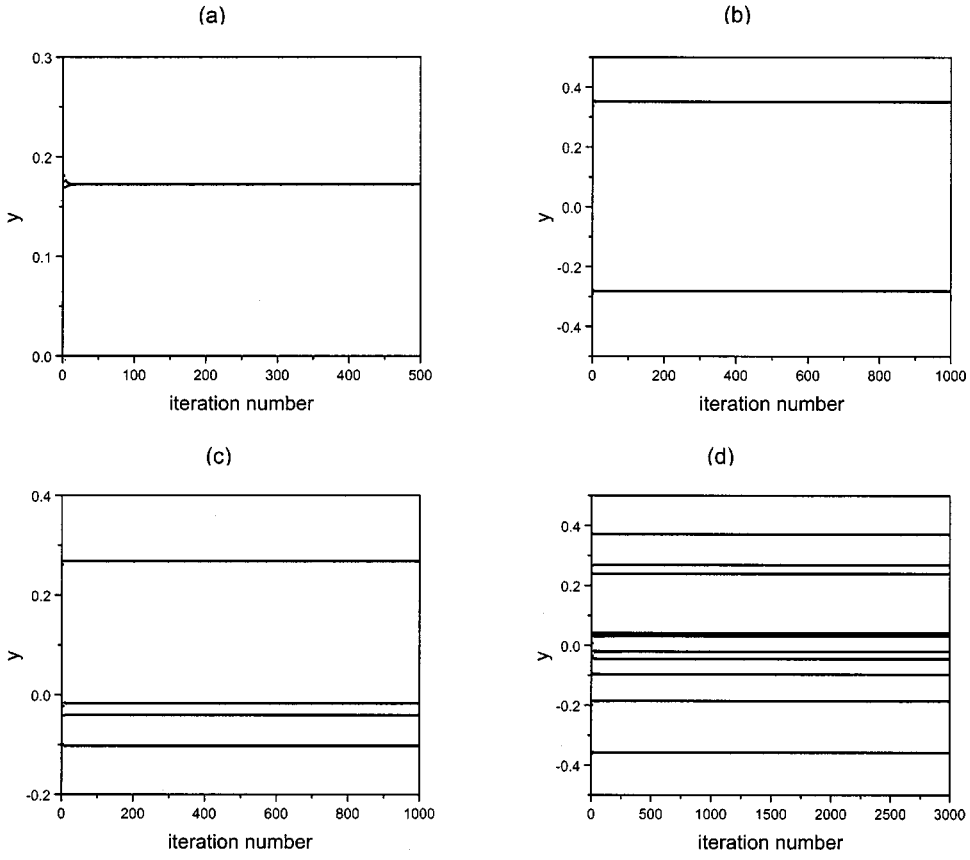

FIG. 2. The four periodic orbits for the Hénon map controlled by intensities (p_{0_x}, p_{0_y}) of periodic pulses. (a) 1; (b) 2; (c) 4; (d) 10.

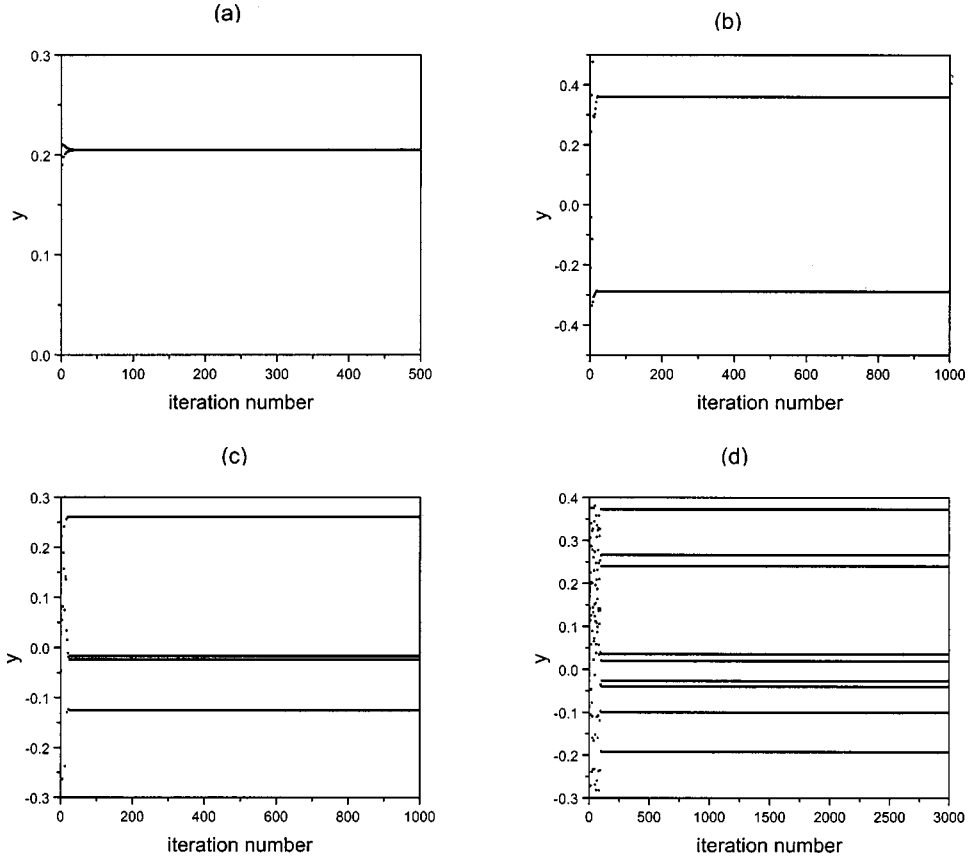

FIG. 3. The four periodic orbits for the Hénon map controlled by intensities (p_x, p_y) of periodic pulses. (a) 1; (b) 2; (c) 4; (d) 10.

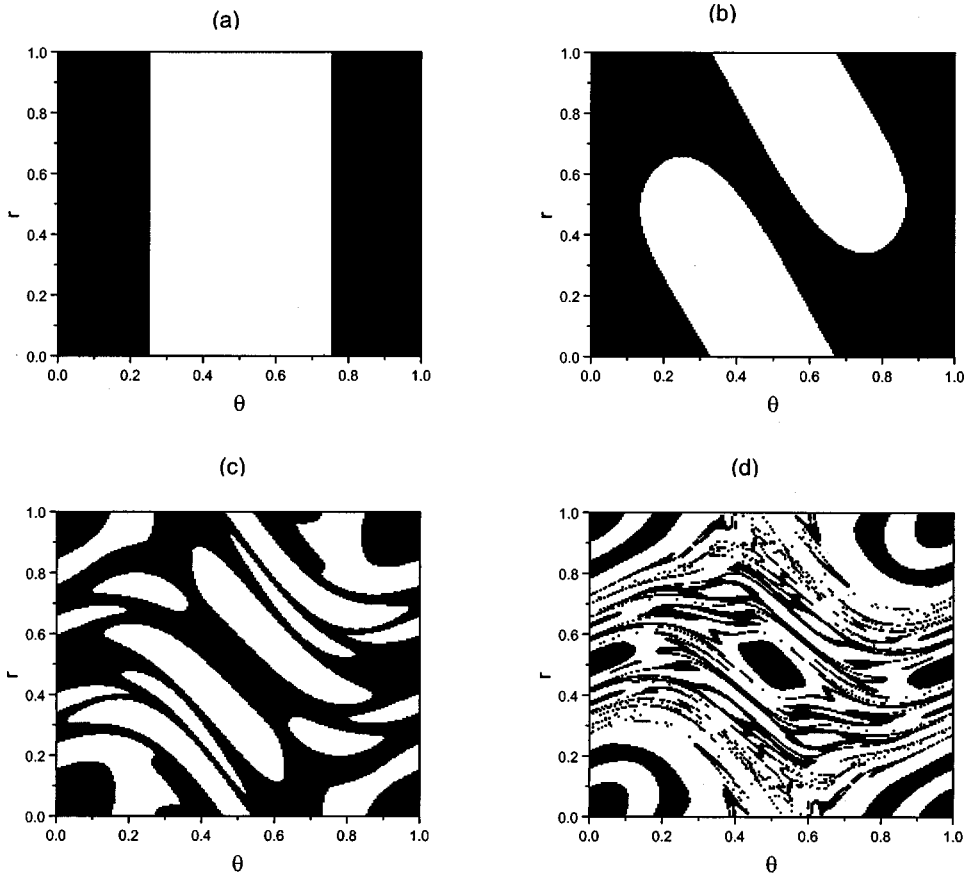

FIG. 4. The finite time convergence zones of different iterations for the standard map. (a) 1; (b) 2; (c) 4; (d) 10.

where m_0 is the initial time of the perturbation. Obviously, $\mathbf{x}_s$ is a fixed point of the map. Because the map does not change the stability of the original map (1), the first T points form a stable period-T orbit.

However, two cases often occur in practice for which the stable periodic orbit may deviate from the one selected. (i) For a system in the neighborhood of $\mathbf{x}_{s+T}$, if we use the perturbation $\mathbf{p}_0$ determined by Eq. (6), the system can only return to the neighborhood of $\mathbf{x}_s$ and not to $\mathbf{x}_s$ exactly. (ii) For a system of T iterations from $\mathbf{x}_s$ (i.e., a system in $\mathbf{x}_{s+T}$), if we use a perturbation $\mathbf{p}$ a little smaller or larger than $\mathbf{p}_0$, the system can also return to the neighborhood of $\mathbf{x}_s$ but in not to $\mathbf{x}_s$. For dissipative systems, an orbit near the stable orbit tends to approach the stable orbit gradually. When the system enters into the neighborhood of the end point we perturbate the system variables to make it return to the neighborhood of the initial point. Thus the system can be stabilized into the desired periodic orbit after only a few iterations. For conservative systems, because the volume of phase space is constant and thus there are no attractors, the stable periodic orbit cannot be obtained in these two cases. What we obtain is a quasiperiodic orbit surrounding the fixed points of the stable period-T orbit. If we want to stabilize the system into the periodic orbit, we need to search for the periodic fixed points corresponding to $\mathbf{p}$. We rewrite Eq. (7) in the form

$$\mathbf{x}^*_{s+T}=(\mathbf{x}_{s+T}+\mathbf{p}+\mathbf{x}_s)/2\approx\mathbf{x}_s\,. \tag{9}$$

Then we can obtain a stable periodic orbit by the action of successive periodic pulses. Of course, the process of looking for the fixed points has changed the conservative property of the system temporarily, but the final stable system is still conservative.

The method can be generalized to continuous time dynamical systems. We may write the equations describing the system in the iterative form by employing a fourth-order Runge-Kutta method,

$$\delta\mathbf{x}_{n+1}=J_n\delta\mathbf{x}_n\,. \tag{10}$$

Here the step length has been carefully chosen in order to avoid spurious behavior. The behavior of the system will be simplified by constructing the proper Poincaré section. The period is defined as the interval between two successive crossings of the section by the orbit from the same side. If a period-N orbit is to be controlled, the perturbation will be acted on the system variables every N times that the orbit

TABLE II. The initial points, end points, and intensities of periodic pulses for four different orbits of the standard map.

T	θ_s	r_s	θ_{s+T}	r_{s+T}	p_θ	p_r
1	0.100	0.700	0.697 10	0.597 10	−0.550	0.080
2	0.650	0.150	0.296 04	0.354 41	0.320	−0.180
4	0.600	0.070	0.429 12	0.082 98	0.160	0.000
10	0.415	0.300	0.617 46	0.286 89	−0.190	−0.010

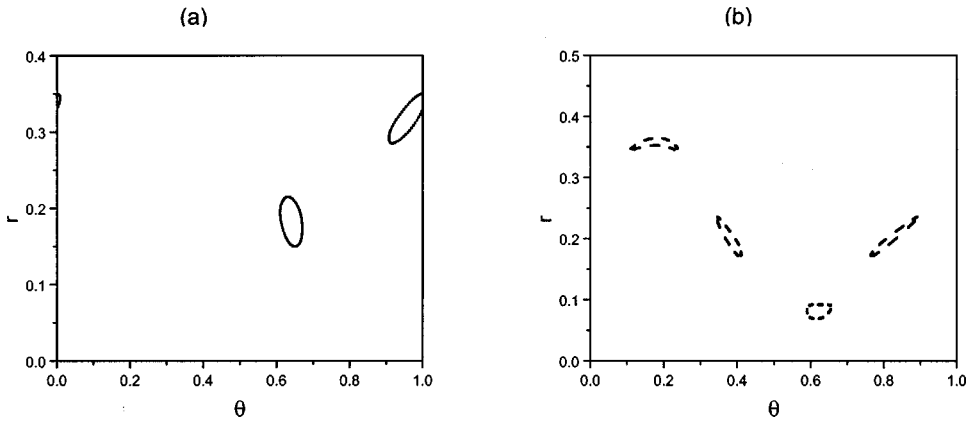

FIG. 5. The quasiperiodic orbits for the standard map controlled by intensities (p_θ, p_r) of periodic pulses surrounding the fixed points of (a) the period-2 and (b) the period-4 orbit.

crosses the Poincaré section from the same side. By repeating the above process, a stable period-N orbit can be obtained.

III. SPECIFIC APPLICATIONS

A. The Hénon map

As an example of a dissipative system, we consider the Hénon map [13]

$$(x_{n+1}, y_{n+1}) = (1 - a x_n^2 + y_n, b x_n), \tag{11}$$

where $a = 1.4$ and $b = 0.3$. The system has a chaotic attractor.

Let an arbitrary point of phase space (x,y) be the initial point. We calculate the finite time Lyapunov exponent for a segment of the chaotic orbit at a given iteration time, and select points that satisfy $\Lambda_i \leqslant 0$, i.e., the finite time convergence zone. Figure 1 shows the finite time convergence zones of different iterations for the Hénon map. Except for one iteration, the areas of the convergence zones decrease as the iteration times increase.

Table I shows the initial points (x_s, y_s), end points (x_{s+T}, y_{s+T}) and intensities (p_{0_x}, p_{0_y}) and (p_x, p_y) of periodic pulses for four different orbits. For case (i) in Sec. II, when the system enters the neighborhood of (x_{s+T}, y_{s+T}), we cause a perturbation (p_{0_x}, p_{0_y}) to act on the system variables to make it return to the neighborhood of (x_s, y_s). Figure 2 shows the stabilized orbits controlled by the intensities (p_{0_x}, p_{0_y}) of periodic pulses. For the case (ii) in Sec. II, when the system is iterated T times starting from the initial point, we cause a perturbation (p_x, p_y) to act on the system vari-

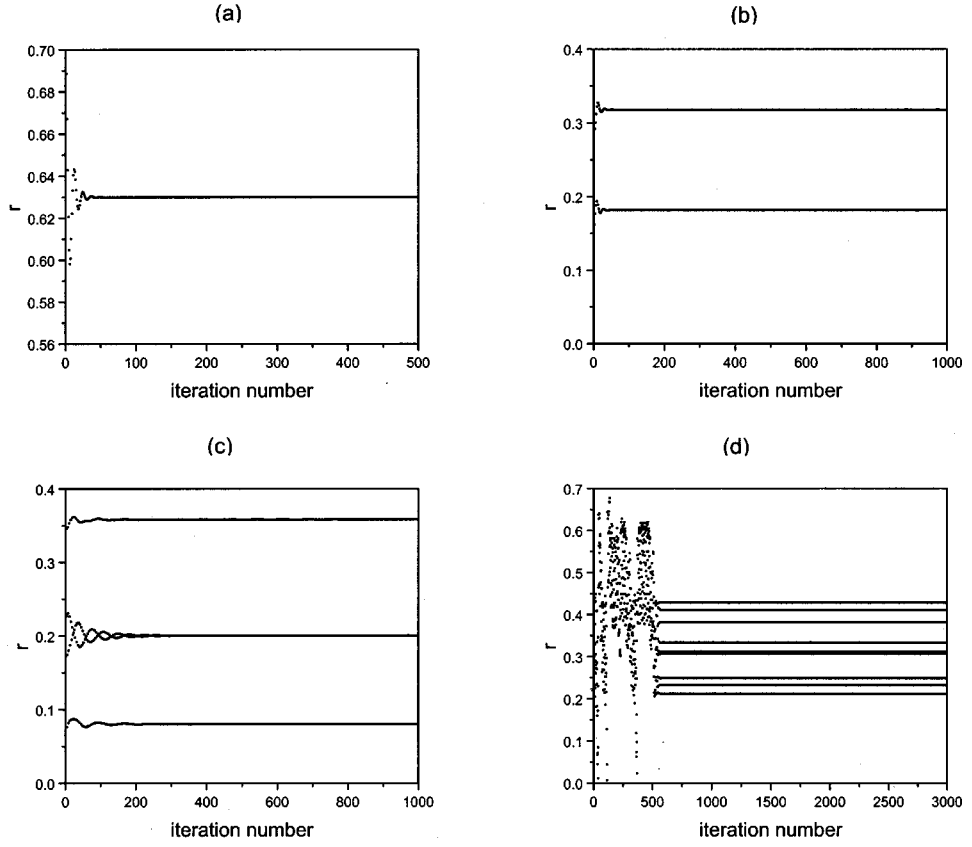

FIG. 6. The four periodic orbits for the standard map controlled by intensities (p_θ, p_r) of periodic pulses. (a) 1; (b) 2; (c) 4; (d) 10.

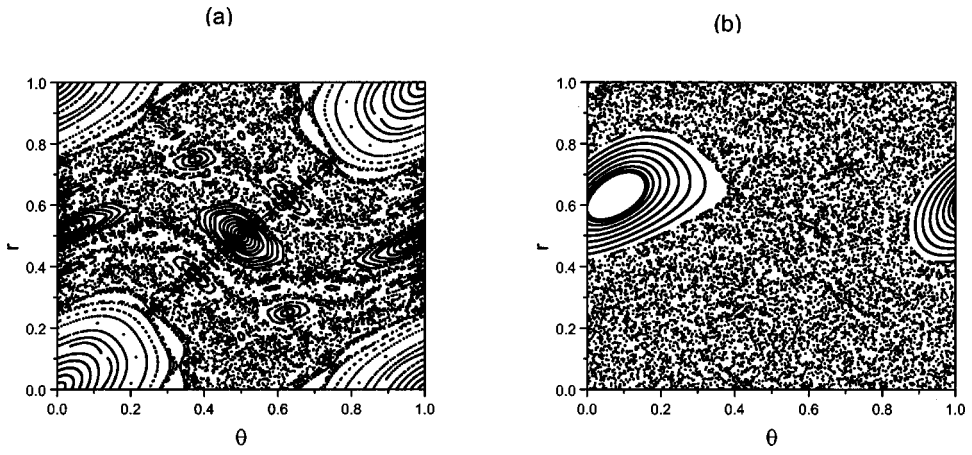

FIG. 7. The phase portraits corresponding to the standard map (a) with $k=1.1$, and (b) controlled by the intensity $(-0.550,0.080)$ of the periodic pulse when $T=1$.

ables to make it return to the neighborhood of (x_s, y_s). Figure 3 shows the stabilized orbits controlled by the intensities (p_x, p_y) of periodic pulses.

B. The standard map

The form of the standard map is [14]

$$(r_{n+1}, \theta_{n+1}) = \left(r_n - \frac{k}{2\pi} \sin(2\pi\theta_n), \theta_n + r_{n+1} \right) \pmod 1 \tag{12}$$

where r and θ are the action and angle coordinates. From the standard map, we can obtain a very clear picture of the mechanisms involved in the transition to global chaos in conservative systems.

Generally, the map exhibits three types of orbit: periodic, quasiperiodic, and chaotic. For $k=0$, the map is integral. With increasing k, the map undergoes a transition from local to global chaos. Above the value of $k=k_c$ ($k_c=0.971\,635\,4$ is called the critical value), the last remaining Kolmogorov-Arnol'd-Moser torus, which stretches horizontally from $x=0$ to 1.0, is broken. For values of $k \leqslant k_c$, it is not possible for any trajectory to diffuse vertically through this line and reach arbitrarily large values of r. For values of $k > k_c$, the system demonstrates global chaos. In this subsection, we

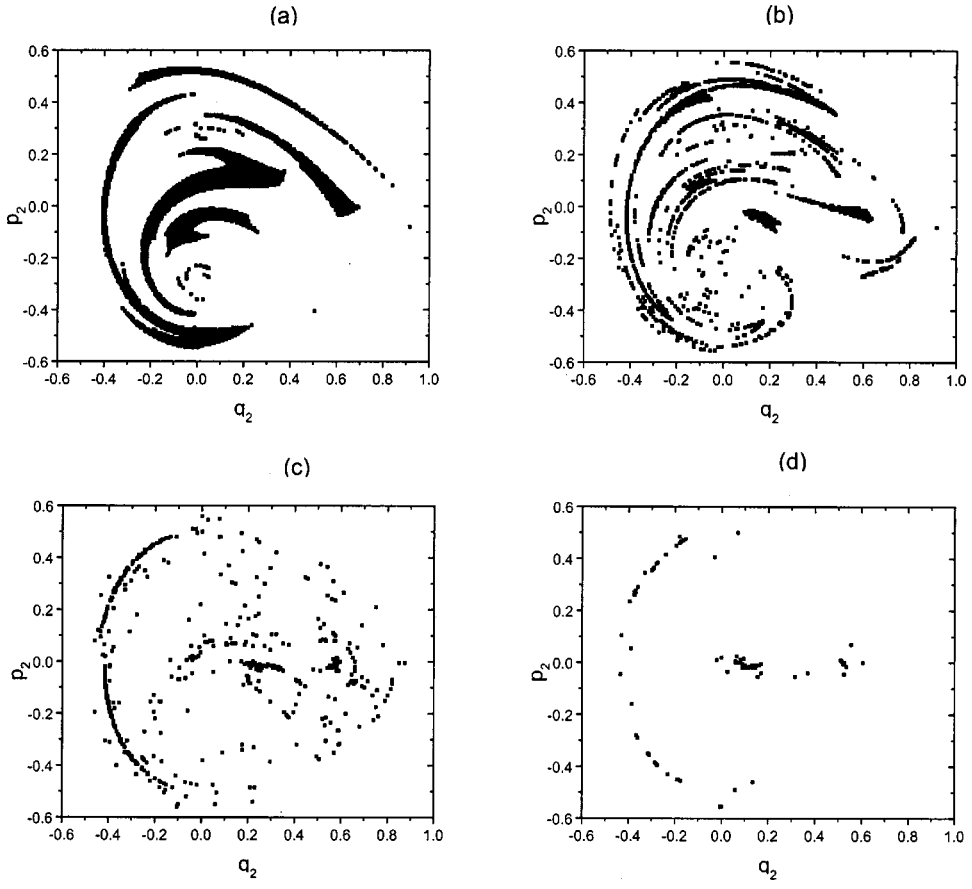

FIG. 8. The finite time convergence zones of different periods for the Hénon-Heiles model. (a) 1; (b) 2; (c) 4; (d) 10.

TABLE III. The initial points, end points, and intensities of periodic pulses on the Poincaré section for four different orbits in the Hénon-Heiles model.

T	q_{2_s}	p_{2_s}	$q_{2_{s+T}}$	$p_{2_{s+T}}$	p_{q_2}	p_{p_2}
1	0.015	−0.230	0.012 21	−0.261 55	0.010	0.020
2	0.135	−0.020	0.108 52	0.020 67	0.010	−0.020
4	0.580	−0.020	0.590 13	0.012 56	0.010	−0.020
10	−0.185	−0.450	−0.156 52	−0.473 11	−0.010	0.010

consider the case of $k=1.1$. As for the Hénon map, we obtain the finite time convergence zones of different iterations as shown in Fig. 4.

The situation of an extremely long chaotic transient when controlling conservative chaos is fundamentally different from the situation of controlling dissipative chaotic attractors [7]. The system needs an extremely long time to reach the neighborhood of the end point, so we study only the second case (ii) in Sec. II. Table II shows the initial points (θ_s, r_s), end points (θ_{s+T}, r_{s+T}), and intensities (p_θ, p_r) of periodic pulses for four different orbits. In the process of control, when the system has iterated T times starting from the initial point, we cause a perturbation (p_θ, p_r) to act on the system variables to make it return to the neighborhood of (θ_s, r_s). For conservative systems, because the volume of phase space is constant and thus there are no attractors, we cannot obtain the selected stable periodic orbits. What we obtain is a quasiperiodic orbit surrounding the fixed points of the stable period-T orbit. Figure 5 shows the quasiperiodic orbits surrounding the fixed points of the period-2 and period-4 orbits. If we want to stabilize the system into the periodic orbit, we need to search for the periodic fixed points corresponding to **p**. Figure 6 shows the stabilized orbits controlled by the intensities (p_θ, p_r) of the periodic pulses in Table II. The numerical results show that orbits starting from convergence zones can be stabilized into the desired periodic orbits rapidly after controlling.

Figure 7(a) shows some orbits for the standard map with $k=1.1$, and Fig. 7(b) shows some orbits for the standard map controlled by the intensity $(-0.550, 0.080)$ of the periodic pulse when $T=1$ [i.e., the global portrait of Fig. 6(a)]. The two phase portraits are completely different. In Fig. 7(b), the resonance zone surrounding the fixed point of the period-1 orbit is clearly seen while the same region is chaotic in Fig. 7(a), and the phase portrait contains a single chaotic orbit except for the resonance zone surrounding the fixed point of the period-1 orbit.

The standard map describes the motion of a periodically kicked rotor. The corresponding Hamiltonian is [14]

$$H(r,\theta,t)=\frac{1}{2}r^2+\frac{k}{(2\pi)^2}\cos(2\pi\theta)\sum_{m=-\infty}^{\infty}\delta(t-m). \tag{13}$$

The Hamiltonian is a function of t; in other words, the sys-

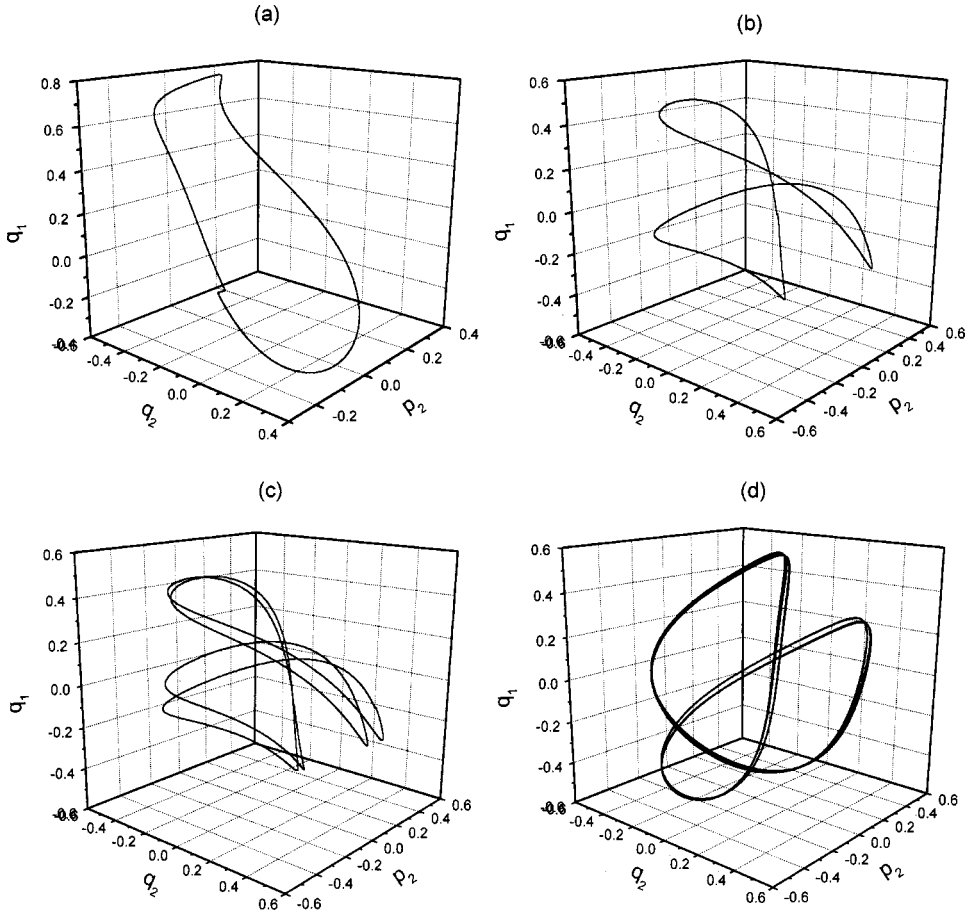

FIG. 9. The four periodic orbits for the Hénon-Heiles model controlled by intensities (p_{q2}, p_{p2}) of periodic pulses. (a) 1; (b) 2; (c) 4; (d) 10.

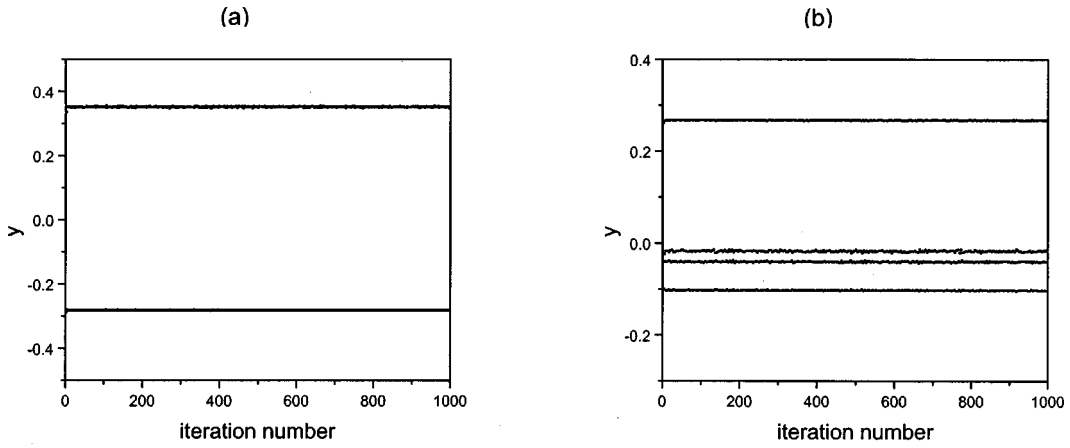

FIG. 10. The effect of additive noise for the Hénon map with $\rho=1.0\times10^{-3}$.

tem energy varies with t. The perturbations may keep the energy balance in a period of the periodically kicked force. So the orbits of the rotor in phase space can be controlled to periodic orbits.

C. The Hénon-Heiles model

The Hénon-Heiles model is a two-dimensional near-integrable Hamiltonian system, and its Hamiltonian is [15]

$$H=\tfrac{1}{2}(p_1^2+p_2^2)+\tfrac{1}{2}(q_1^2+q_2^2)+q_1^2q_2-\tfrac{1}{3}q_2^3. \tag{14}$$

The canonical equations are

$$\begin{aligned}\frac{dq_1}{dt}&=p_1,\\ \frac{dq_2}{dt}&=p_2,\\ \frac{dp_1}{dt}&=-q_1-2q_1q_2,\\ \frac{dp_2}{dt}&=-q_2-q_1^2-q_2^2.\end{aligned} \tag{15}$$

The energy is conserved and this restricts the trajectories to lie on a three-dimensional surface in the four-dimensional phase space. We take the section (q_2,p_2) at $q_1=0$ with $p_1>0$ to be a Poincaré section. For a given (q_2,p_2), p_1 is

$$p_1=(2E-p_2^2-q_2^2+\tfrac{2}{3}q_2^3)^{1/2}. \tag{16}$$

In this section, we set the energy to be $E=0.166\,67$. Periodic and quasiperiodic orbits hardly exist, and a single trajectory almost fills the whole isoenergetic surface.

According to the above control method, we rewrite Eq. (15) in iterative form by employing a fourth-order Runge-Kutta method where the step length is $h=0.1$:

$$\begin{pmatrix}\delta q_{1_{n+1}}\\ \delta q_{2_{n+1}}\\ \delta p_{1_{n+1}}\\ \delta p_{2_{n+1}}\end{pmatrix}=\begin{pmatrix}J_{11}&J_{12}&J_{13}&J_{14}\\ J_{21}&J_{22}&J_{23}&J_{24}\\ J_{31}&J_{32}&J_{33}&J_{34}\\ J_{41}&J_{42}&J_{43}&J_{44}\end{pmatrix}\begin{pmatrix}\delta q_{1_n}\\ \delta q_{2_n}\\ \delta p_{1_n}\\ \delta p_{2_n}\end{pmatrix}, \tag{17}$$

where (J_{ij}) is a Jacobian matrix. We obtain J to an accuracy of h^4:

$$J_{11}=1-\frac{h^2}{2}-h^2q_2-\frac{h^3}{3}p_2+\frac{h^4}{24}+\frac{h^4}{4}q_2+\frac{h^4}{4}q_1^2+\frac{h^4}{12}q_2^2,$$

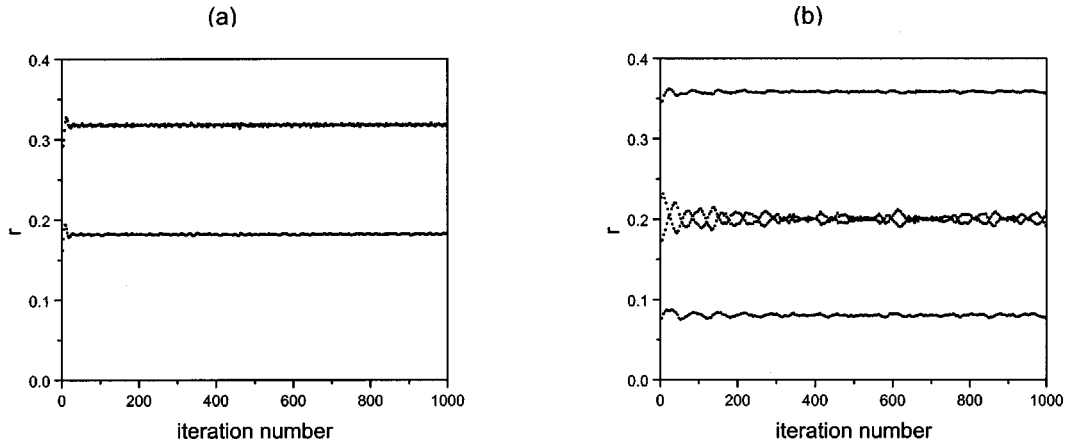

FIG. 11. The effect of additive noise for the standard map with $\rho=5.0\times10^{-4}$.

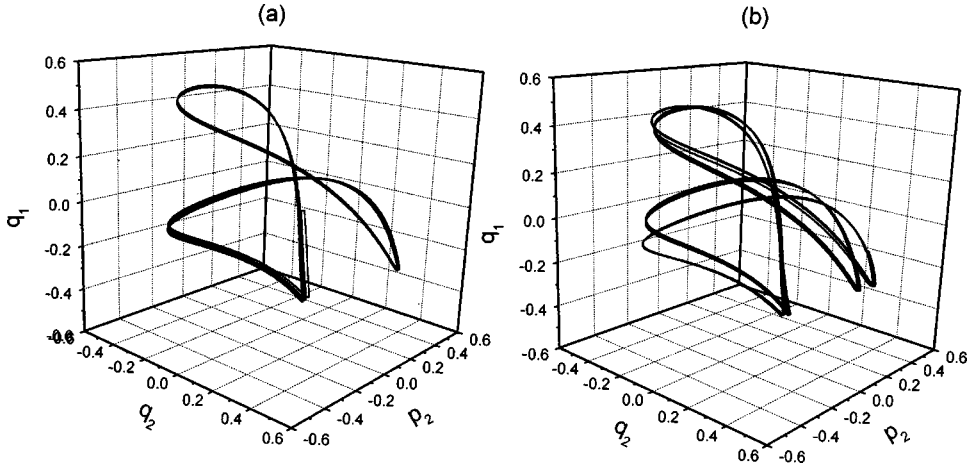

FIG. 12. The effect of additive noise for the Hénon-Heiles model with $\rho=$(a)5.0×10^{-5} and (b) 2.0×10^{-5}.

$$J_{12}=-h^2q_1-\frac{h^3}{3}p_1+\frac{h^4}{4}q_1+\frac{h^4}{6}q_1q_2,$$

$$J_{13}=h-\frac{h^3}{6}-\frac{h^3}{3}q_2-\frac{h^4}{6}p_2,$$

$$J_{14}=-\frac{h^3}{3}q_1-\frac{h^4}{6}p_1,$$

$$J_{21}=-h^2q_1-\frac{h^3}{3}p_1+\frac{h^4}{4}q_1+\frac{h^4}{6}q_1q_2,$$

$$J_{22}=1-\frac{h^2}{2}+h^2q_2+\frac{h^3}{3}p_2+\frac{h^4}{24}-\frac{h^4}{4}q_2+\frac{h^4}{12}q_1^2+\frac{h^4}{4}q_2^2,$$

$$J_{23}=-\frac{h^3}{3}q_1-\frac{h^4}{6}p_1,$$

$$J_{24}=h-\frac{h^3}{6}+\frac{h^3}{3}q_2+\frac{h^4}{6}p_2,$$

$$J_{31}=-h-2hq_2-h^2p_2+\frac{h^3}{6}+h^3q_2+h^3q_1^2+\frac{h^3}{3}q_2^2+\frac{5h^4}{12}p_2+\frac{5h^4}{6}q_1p_1+\frac{h^4}{2}q_2p_2,$$

$$J_{32}=-2hq_1-h^2p_1+h^3q_1+\frac{2h^3}{3}q_1q_2+\frac{5h^4}{12}p_1-\frac{h^4}{6}q_2p_1+\frac{h^4}{2}q_1p_2,$$

$$J_{33}=1-\frac{h^2}{2}-h^2q_2-\frac{2h^3}{3}p_2+\frac{h^4}{24}+\frac{5h^4}{12}q_2+\frac{5h^4}{12}q_1^2-\frac{h^4}{12}q_2^2,$$

$$J_{34}=-h^2q_1-\frac{2h^3}{3}p_1+\frac{5h^4}{12}q_1+\frac{h^4}{2}q_1q_2,$$

$$J_{41}=-2hq_1-h^2p_1+h^3q_1+\frac{2h^3}{3}q_1q_2+\frac{5h^4}{12}p_1-\frac{h^4}{6}q_1p_2+\frac{h^4}{2}q_2p_1,$$

$$J_{42}=-h+2hq_2+h^2p_2+\frac{h^3}{6}-h^3q_2+\frac{h^3}{3}q_1^2+h^3q_2^2-\frac{5h^4}{12}p_2+\frac{5h^4}{6}q_2p_2+\frac{h^4}{2}q_1p_1,$$

$$J_{43}=-h^2q_1-\frac{2h^3}{3}p_1+\frac{5h^4}{12}q_1+\frac{h^4}{2}q_1q_2,$$

$$J_{44}=1-\frac{h^2}{2}+h^2q_2+\frac{2h^3}{3}p_2+\frac{h^4}{24}-\frac{5h^4}{12}q_2-\frac{h^4}{12}q_1^2+\frac{5h^4}{12}q_2^2.$$

To control a period-N orbit, we can multiply all the Jacobian matrices from the initial point to the Nth piercing point of the section along the trajectory according to Eq. (3). If each eigenvalue of the Jacobian matrix has a real part that is less than or equal to 1, the orbit is stable. Then we can determine the finite time convergence zone on the Poincaré section. Figure 8 shows the finite time convergence zones of different periods. As in the standard map, the areas of the convergence zones decrease as the periods increase.

Table III shows the initial points (q_2,p_2), end points $(q_{2_{s+T}},p_{2_{s+T}})$ and intensities (p_{q_2},p_{p_2}) of periodic pulses on the Poincaré section for four different orbits. In the process of control, when the system falls on the Poincaré section, we cause a perturbation (p_{q_2},p_{p_2}) to act on the system variables to make it return to the neighborhood of (q_{2_s},p_{2_s}). Figure 9 shows the stable orbits controlled by intensities (p_{q_2},p_{p_2}) of the periodic pulses in Table III after discarding the transient process of looking for the periodic fixed points.

For the Hénon-Heiles model, the energy is conserved. In Table III, we give only the perturbations p_{q_2} and p_{p_2} at q_1

$=0$. In fact, the perturbation p_{p_1} also exists. But p_{p_1} is determined by p_{q_2} and p_{p_2} in order that the energy remains constant. In other words, the perturbations are precisely tuned so that the system energy input/output is zero.

IV. EFFECT OF NOISE

An important issue in a method that attempts to stabilize chaotic systems is its robustness against the presence of external noise. In this section, we consider Gaussian white noise generated by using the Box-Muller method [16], and introduce additive noise in the form

$$x_i' = x_i + \rho\xi(t) \quad (i=1,2,\ldots,N), \tag{18}$$

where ρ denotes the intensity of external noise. The noise is applied at each Runge-Kutta integration step,

$$\langle \xi(t) \rangle = 0, \quad \langle \xi(t)\xi(t') \rangle = \delta(t-t'). \tag{19}$$

Figure 10 shows the effect of noise for the period-2 and period-4 orbits corresponding to Fig. 2. The intensity of noise acting on the system variables x and y is $\rho = 1.0\times10^{-3}$. Figure 11 shows the effect of noise for the period-2 and period-4 orbits corresponding to Fig. 6. The intensity of noise acting on the system variables r and θ is $\rho = 5.0\times10^{-4}$. Figure 12 shows the effect of noise for the period-2 and period-4 orbits corresponding to Fig. 9. The intensity of noise acting on the system variables q_2 and p_2 is $\rho = 5.0\times10^{-5}$ for the period-2 orbit and 2.0×10^{-5} for the period-4 orbit. Comparing Fig. 10 with Fig. 2, Fig. 11 with Fig. 6, and Fig. 12 with Fig. 9, we can see that the noisy orbits remain within a small neighborhood of the noise-free orbits and do not wander over the whole phase space. So they are still periodic. This shows that the constant periodic pulse method is robust against external noise. The numerical results also show that the effect of noise is greater for high-periodic than for low-periodic orbits. Further study shows that the effect of noise is related to the position of the initial point. If the initial point is located at the edge of the finite time convergence zone, the system is much more sensitive to noise.

V. CONCLUSION

In this paper, we propose a constant periodic pulse method and successfully illustrate the method with three examples for discrete dissipative, discrete, and continuous conservative systems. The key of the method is to search for the finite time convergence zones in different time lengths, i.e., all the stable segments of the chaotic orbits in different time lengths. Generally, the finite time convergence zones decrease as the periods increase. The constant periodic pulse method is robust against external noise.

Compared with other periodic pulse methods, our control method is aimed at desired dynamical targets with a good diversity. Using the method, we can target not only preexisting periodic orbits in the given system, but also new orbits not naturally visited in the unperturbed dynamics. It is more important that the Jacobian determinant is invariant under the action of the perturbation on the system variables, i.e., that this does not change the conservative property of the system. Therefore, the method is suitable for both dissipative and conservative systems. The behavior of the controlled system is dependent not only on the control parameters (interval and intensity of pulse), but also on the position of the initial point. Further studies are currently in progress.

ACKNOWLEDGMENTS

H.X. thanks Y.X. Cheng for useful discussions. This work was supported by the Special Funds for Major State Basic Research Projects, the National Natural Science Foundation of China, and the Science Foundation of China Academy of Engineering Physics.

[1] E. Ott, C. Grebogi, and J. A. Yorke, Phys. Rev. Lett. **64**, 1196 (1990).
[2] Y. Braiman and I. Goldhirsch, Phys. Rev. Lett. **66**, 2545 (1991).
[3] E. R. Hunt, Phys. Rev. Lett. **67**, 1953 (1991).
[4] E. A. Jackson, Phys. Lett. A **151**, 478 (1990).
[5] M. A. Matias and J. Guemez, Phys. Rev. Lett. **72**, 1455 (1994).
[6] N. P. Chau, Phys. Rev. E **57**, 378 (1998).
[7] Y. C. Lai, M. Ding, and C. Grebogi, Phys. Rev. E **47**, 86 (1993).
[8] Z. Wu, Z. Zhu, and C. Zhang, Phys. Rev. E **57**, 366 (1998).
[9] A. Oloumi and D. Teycheme, Phys. Rev. E **60**, R6279 (1999).
[10] C. Ziehmann, L. A. Smith, and J. Kurths, Physica D **126**, 49 (1999).
[11] Y. X. Cheng, S. G. Chen, and G. R. Wang, Chin. Sci. Bull. **40**, 1746 (1995).
[12] H. D. I. Abarbanel, R. Brown, and M. B. Kenel, J. Nonlinear Sci. **1**, 175 (1991).
[13] M. Hénon, Commun. Math. Phys. **50**, 69 (1976).
[14] B. V. Chirikov, Phys. Rep. **52**, 263 (1979).
[15] L. J. Reichl, *The Transition to Chaos* (Springer-Verlag, New York, 1992), p. 28.
[16] B. Shraiman, C. E. Wayne, and P. C. Martin, Phys. Rev. Lett. **46**, 935 (1981).